Shifting Electronic Structure by Inherent Tension in Molecular Bottlebrushes with Polythiophene Backbones

Yuanchao Li,[†] Alper Nese,[‡,§] Xiangqian Hu,[∥] Natalia V. Lebedeva,[†] Travis W. LaJoie,[†] Joanna Burdyńska,[‡] Mihaela C. Stefan,[‡,§] Wei You,[†] Weitao Yang,[∥] Krzysztof Matyjaszewski,[‡] and Sergei S. Sheiko*,[†]

[†]Department of Chemistry, University of North Carolina at Chapel Hill, North Carolina 27599, United States
[‡]Department of Chemistry, Carnegie Mellon University, 4400 Fifth Avenue, Pittsburgh, Pennsylvania 15213, United States
[∥]Department of Chemistry, Duke University, Durham, North Carolina 27708, United States

S *Supporting Information*

ABSTRACT: Bottlebrush macromolecules can be regarded as molecular tensile machines, where tension is self-generated along the backbone due to steric repulsion between densely grafted side chains. This intrinsic tension is amplified upon adsorption of bottlebrush molecules onto a substrate and increases with grafting density, side chain length, and strength of adhesion to the substrate. To investigate the effects of tension on the electronic structure of polythiophene (PT), bottlebrush macromolecules were prepared by grafting poly(n-butyl acrylate) (PBA) side chains from PT macroinitiators by atom transfer radical polymerization (ATRP). The fluorescence spectra of submonolayers of PT bottlebrushes were measured on a Langmuir–Blodgett (LB) trough with the backbone tension adjusted by controlling the side-chain length, surface pressure, and chemical composition of a substrate. The wavelength of maximum emission has initially red-shifted, followed by a blue-shift as the backbone tension increases from 0 to 2.5 nN, which agrees with DFT calculations. The red-shift is ascribed to an increase in the conjugation length due to the extension of the PT backbone at lower force regime (0–1.0 nN), while the blue-shift is attributed to deformations of bond lengths and angles in the backbone at higher force regime (1.0–2.5 nN).
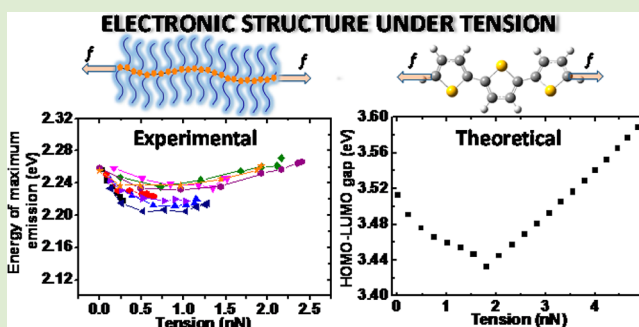
M aterials may change color upon mechanical deformation.[1] This can occur due to conformational transitions,[2] formation of excimers,[3,4] dissociation of chromophore aggregates,[5,6] and generation of electrostatic charges.[7] Correspondingly, light can be used to cause deformation[8] and scission[9−12] of covalent bonds. Due to uneven distribution of strain in macroscopic samples, molecular-scale experiments have been developed to monitor the effect of strain on the electronic structure of specific chemical groups.[13−17] Typically, molecules are stretched by an external stimulus including direct[18,19] and inductive[20,21] force application. In contrast to the previous studies, we have developed bottlebrush macromolecules that self-generate significant tension of the order of 1 nN,[22,23] which is sufficient for breaking strong covalent bonds.[24−27] One unique feature of this system is that the bottlebrush backbone is under controlled tension imposed by steric repulsion between the densely grafted side chains. By adjusting molecular architecture (side chain length and grafting density) and environmental conditions (solvent quality and temperature), we can vary the backbone tension in a range from 1 pN to 1 nN. Through insertion of chromophores into the bottlebrush backbone, these molecular tensile machines are well-suited for studies of the effect of mechanical tension on electronic structure of covalent bonds. Unlike the above-mentioned studies of spectroscopic changes due to bond

scission and conformational transitions, we want to understand the implications of strained covalent bonds and angles.

In this communication, we report the effect of mechanical tension on the photophysical properties of molecular bottlebrushes with polythiophene (PT) backbones. Polythiophene was chosen for this study because of well-studied correlations between its π-conjugated structure and electro-optical properties. PT is commonly used in photovoltaic cells,[28] field-effect transistors,[29] and is a very popular material for molecular wire applications[30] and light-emitting diodes.[31] Therefore, understanding the effect of mechanical tension on the photophysical properties of polythiophene may have interesting implications for flexible organic electronics.[32]

Polymer bottlebrushes with a regiorandom polythiophene backbone were synthesized using the atom transfer radical polymerization (ATRP) technique.[33−35] A polythiophene-based macroinitiator (MI), was reacted with n-butyl acrylate (BA) under typical ATRP conditions (Supporting Information). Five bottlebrushes were prepared, with degrees of polymerization (DPs) of poly(n-butyl acrylate) (PBA) side

chains of 5, 25, 60, 120, and 190. These bottlebrushes are coded as PT-*m*, where *m* is the DP of the PBA side chains. To confirm the successful synthesis of the PT bottlebrushes, we used atomic force microscopy (AFM) aiming at imaging of individual molecules. As shown in Figure 1, the imaged
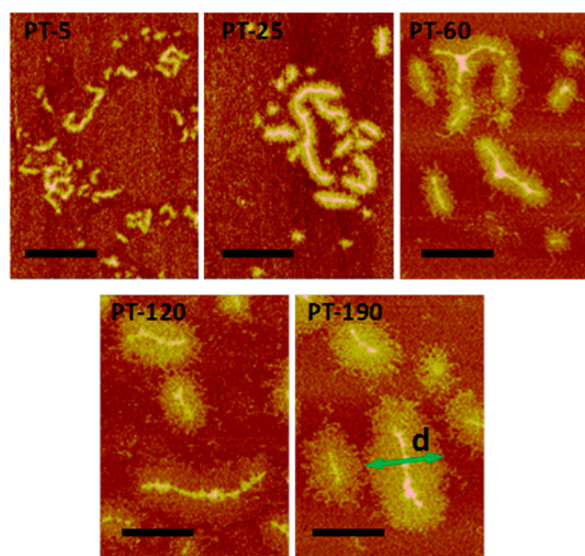
Figure 1. AFM height images of the PT bottlebrushes with different DP values of PBA side chains spin-cast from dilute chloroform solution onto freshly cleaved mica substrates. The scale bar is 150 nm.

molecules exhibit wormlike conformations, suggesting extension of bottlebrush backbone. The width of the molecular bottlebrushes increases with the DP of PBA side chains (Table 1).

Table 1. Characterization of PT Bottlebrushes

sample	$M_n{}^a$	$Đ^b$	d^c (nm)
MI	46200	11.6^d	NA
PT-5	135000	5.0	15 ± 3
PT-25	244000	4.5	35 ± 2
PT-60	643000	2.9	64 ± 2
PT-120	852000	2.6	84 ± 2
PT-190	1040000	2.5	120 ± 2

[a]Molecular weight determined by GPC using poly(methyl methacrylate) standard. [b]Dispersity determined by GPC. [c]The width of PT bottlebrushes measured by AFM (Figure 1). [d]The substantial decrease in the dispersity of PT bottlebrushes with respect to MI is ascribed to better solubility of brushes and potential fractionation at each separation stage.

To investigate tension effects on the photophysical properties of the PT bottlebrushes, we have constructed an apparatus enabling measurements of fluorescence spectra of submonolayer films deposited at a liquid−air interface. Specifically, we have integrated a Langmuir−Blodgett (LB) trough with a quartz window, an inverted optical microscope, and a spectrograph (Figure 2a, see Supporting Information for description of the apparatus).

As discussed elsewhere, adsorption of densely grafted side chains have multiple effects on arrangement of bottlebrush molecules at interfaces, resulting in concurrent extension, separation, and alignment of bottlebrush backbones.[36] This causes coplanar orientation of the backbone and prevents
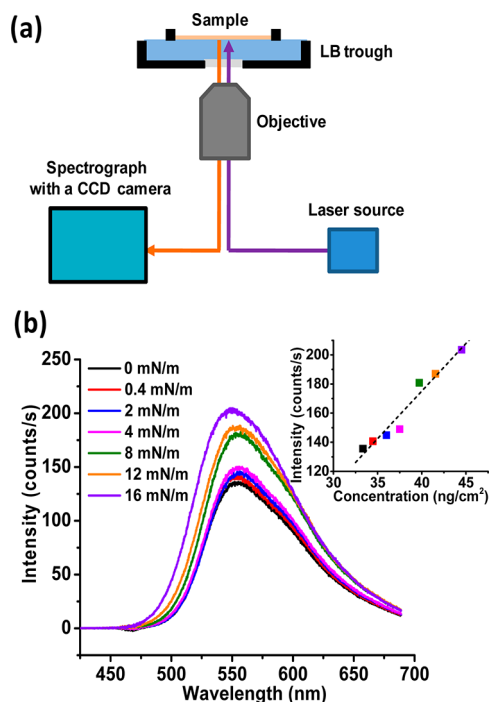
Figure 2. (a) Schematic representation of the fluorescence spectroscopy setup. (b) Fluorescence spectra of PT-120 on a 0.5% w/w 2-propanol substrate at various surface pressures (excitation at 405 nm). Inset: plot of maximum intensity vs PT-120 concentration at different surface pressures, dashed line is a linear fit.

intermolecular interactions between neighboring PT chains. In addition, the introduction of side chains results in two counteracting effects on the fluorescence intensity of PT bottlebrushes. On one hand, adsorption of side chains reduces submonolayer concentration of thiophene units. For example, monolayer of PT-120 at 8 mN/m corresponds to a PT surface concentration of ∼2 ng/cm² and surface fraction of thiophene monomeric units of ∼0.05 nm⁻². On the other hand, the emission intensity of bottlebrush monolayers was about 50× higher than that for MI at the same surface fraction of thiophene units (Figure S1 in Supporting Information). This effect is attributed to the screening of PT backbones by the densely grafted side chains and thus suppression of energy transfer to the neighboring chains.[37,38] In sum, we have acquired decent fluorescence spectra of the PT bottlebrush films under controlled bond tension with a signal-to-noise ratio of ∼10^3 even for PT-190 that has the lowest concentration of thiophene units.

As a representative example, Figure 2b shows fluorescence spectra of PT-120, adsorbed onto a 0.5% w/w 2-propanol substrate, under controlled surface pressures from 0 to 16 mN/m. At low surface pressures promoting strong interaction of the bottlebrushes with the substrate, the spectra exhibit a peak at ∼550 nm and a shoulder at ∼600 nm, while at high surface pressures, the shoulder becomes less pronounced. This can be attributed to planarization of the PT backbone due to stretching as a result of spreading on the substrate.[38] The emission intensity increases with the surface pressure due to the increase in surface concentration of PT-120 molecules upon compression. The inset in Figure 2b shows linear increase of maximum intensity with PT-120 concentration, which indicates that the fluorescence intensity per thiophene unit remains constant at different surface pressures. In addition to the

intensity variations, we have also measured small shifts of the maximum emission ($\lambda_{max,em}$), depending on the surface pressure, which is directly related to backbone tension[23] as discussed below.

Fluorescence spectra may exhibit significant changes due to many reasons including both chemical and physical environments of fluorophores, for example, covalent linkers, solvent molecules, and concentration, which could account for the discrepancy in the energy of maximum emission at the same backbone tension for different data sets. To verify the spectroscopic shifts and to localize the effect of tension apart from the other effects, three complementary methods have been used to control the backbone tension. As shown previously,[22,23] the tension along the backbone in molecular bottlebrushes adsorbed to a flat substrate can be expressed as $f \cong S \cdot d$ at zero surface pressure ($\Pi = 0$), where d is the width of the adsorbed bottlebrushes (Figure 1). The spreading parameter $S = \gamma_{sg} - (\gamma_{sl} + \gamma_{lg})$ is the difference between the interfacial energies for the substrate/gas (sg), substrate/liquid (sl), and liquid/gas (lg) interfaces. The spreading parameter was determined from the surface pressure-molecular area isotherms measured at high compressions.[39,40] At nonzero surface pressure, the expression for f can be modified as:

$$f \cong (S - \Pi) \cdot d$$

This equation implies that there are three ways to control the backbone tension: (i) surface energy of the subphase (2-propanol addition), (ii) lateral compression, and (iii) side chain length. The surface energy of the subphase can be reduced by adding 2-propanol into water, leading to a decrease in the spreading parameter S and, correspondingly, the scission rate of the backbone. Lateral compression allows accurate control of the surface pressure, whereas higher compression results in a lower backbone tension. A systematic series of five PT bottlebrushes with different DPs of side chains allows precise control of the backbone tension.

To quantify the spectroscopic shifts as a function of the backbone tension, we have calculated the energy of maximum emission using the equation $E_{max,em} = \hbar c / \lambda_{max,em}$, where $\hbar$ is the normalized Planck's constant and c is the speed of light. Figure 3a shows a representative example of the normalized spectra of PT-60 adsorbed onto a 0.5% w/w 2-propanol substrate at different surface pressures as well as the corresponding $E_{max,em}$ as a function of backbone tension (inset). We focused on the emission spectra of the same PT bottlebrush on the same substrate; the only change was due to surface pressure, while the PT backbones remain isolated inside the shell of PBA side chains. As shown in Figure 3b, for the same PT bottlebrush on the same substrate (connected data points), the energy of maximum emission decreases with increasing backbone tension below a certain threshold (ca. 1 nN); beyond the threshold tension, the energy of maximum emission increases. The same trend is observed for all the samples studied, though the threshold tensions could be slightly different.

To gain insight into our experimental observations, we have used density functional theory (DFT) to calculate the effect of tension on the electronic structure of a model oligomer consisting of three thiophene (3T) monomers (see details in Supporting Information). As show in Figure 4b, the HOMO–LUMO gap of the model oligothiophene shows the same trend as we observed for $E_{max,em}$: it decreases and then increases with applied tension. In addition, the changes in the HOMO–LUMO gap strongly correlate with changes in the dihedral
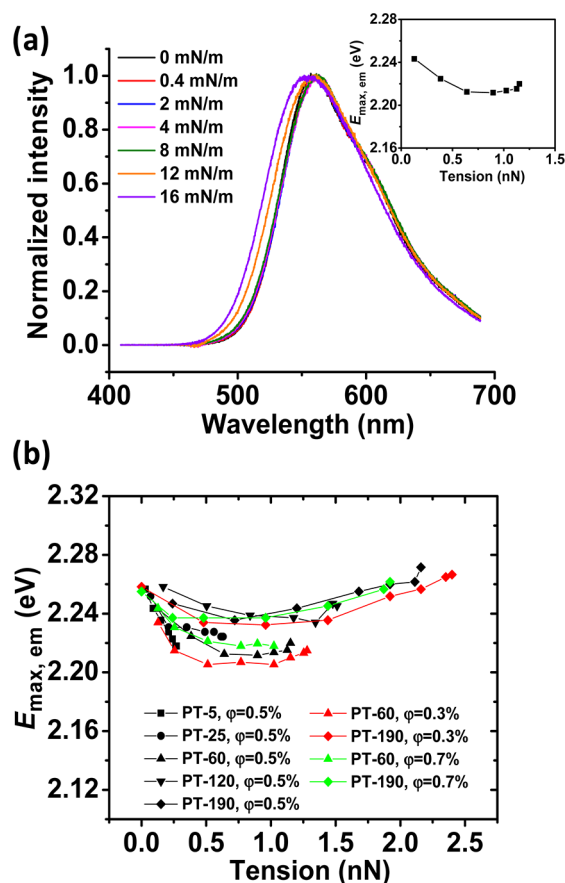
Figure 3. (a) Normalized emission spectra of PT-60 adsorbed on a 0.5% w/w 2-propanol substrate at different surface pressures. Inset: the corresponding energy of maximum emission as a function of backbone tension calculated using the equation $f \cong (S - \Pi) \cdot d$, where the spreading parameter S is 18 mN/m and the brush width d is 64 nm. (b) Changes in the energy of maximum emission of the PT backbone with tension, which was controlled through variation of side chain length on aqueous substrates containing different weight fractions φ of 2-propanol.

angle. As such, the decrease in $E_{max,em}$ (red shift) upon mild increase in backbone tension can be attributed to an increase in conjugation length due to greater planarity of the PT backbone as it becomes more extended (Figure S2).[41] Similar spectroscopic shifts have been observed upon conformational changes in PT backbones of molecular bottlebrushes caused by temperature-induced conformational transition of poly(N-isopropylacrylamide) (PNIPAAm) side chains[42,43] and variations of solvent quality.[44] As the planarity of the PT backbone reaches its limit, molecular deformations of the bond lengths and angles due to larger tension begin to dominate, resulting in the increase of $E_{max,em}$ (blue shift) with backbone tension. In fact, the bond lengths and angles are also deformed before the threshold tension point (Figure 4c,d), but the effect of increasing planarity dominates, leading to a net decrease.
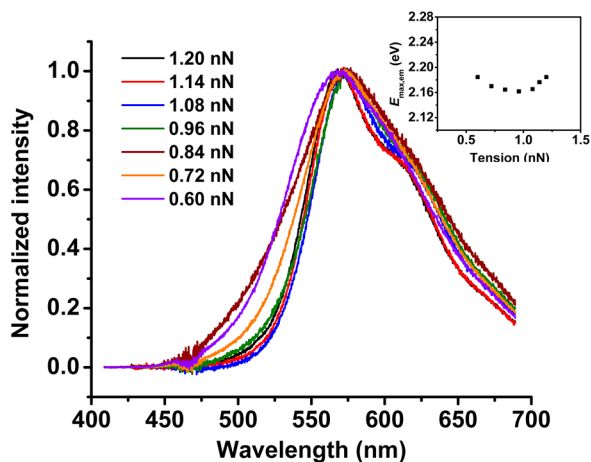
The blue shift in the maximum emission is a more complex phenomenon. Generally, the deformations of bond angles and bond lengths in the backbones disrupt the distribution of electron density within the thiophene rings and over the chain. In other words, the elongation of thiophene-thiophene C–C bonds (e.g., C1–C9) upon stretching the backbone results in increasing π-electron localization within thiophene rings, which
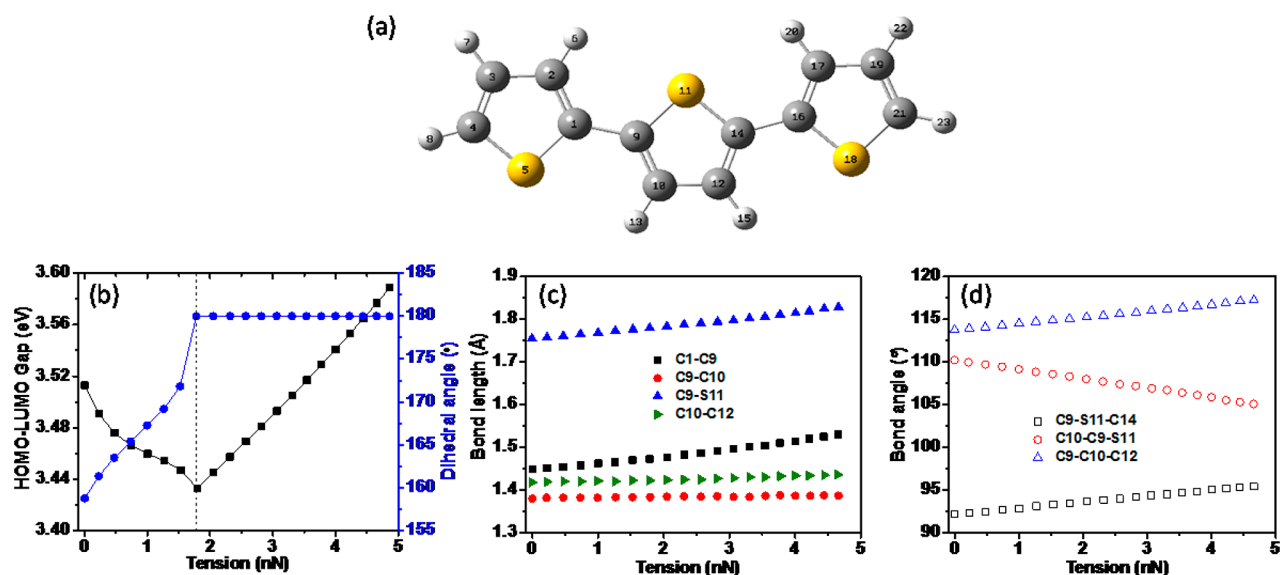
Figure 4. (a) Chemical structure of the model oligothiophene; (b) changes in the HOMO−LUMO gap and the dihedral angle between neighboring thiophene rings with applied tension based on DFT; representative changes in (c) bond lengths and (d) angles with applied tension in the middle thiophene ring.

reduces the overall π-electron delocalization over the whole chain, leading to a blue shift in emission.

Admittedly, the shifts in the energy of maximum emission are small, but still in good agreement with the DFT calculations. The experimental threshold tension (ca. 1 nN) is smaller than that predicted for the fully planar oligothiophene (1.7 nN), which might be attributed to the complex structures of the PT bottlebrush molecules. To gain more insights on the effects of tension on the electronic structure of polythiophene, we tested a molecular bottlebrush with regioregular poly(3-hexylthiophene) backbone (rr-P3HT bottlebrush, see Supporting Information), where steric hindrances between side chains are minimized. As shown in Figure 5, the rr-P3HT bottlebrush followed the same trend as observed for PT bottlebrushes with regiorandom backbones: the energy of maximum emission decreases and then increases as tension increases from 0.6 to 1.2 nN, with a threshold tension of ∼1.0 nN as well. It is worth pointing out that this trend is even more pronounced than in

regiorandom structures in Figure 3. We have also measured UV−vis absorption of PT bottlebrush monolayers using a Cary 60 Spectrophotometer with fiber optics. Unfortunately, a low signal/noise ratio did not allow quantitative interpretation of band-shifts even for PT-5 that had the highest surface fraction of thiophene monomeric units (Figure S6).

In conclusion, we have used polymer bottlebrushes as molecular tensile machines to study the effects of tension on the photophysical properties of PT conjugated polymers. We have been able to measure the emission spectrum of conjugated PT backbones in bottlebrush monolayers at extremely low surface fraction of thiophene monomeric units (ca. 0.05 nm^{-2}) under controlled backbone tension (0−2.5 nN). The maximum emission has initially red-shifted and then blue-shifted with increasing tension due to the increase of conjugation length and the deformations of bond lengths/angles, respectively, which is in good agreement with DFT calculations. This suggests that molecular tension may be utilized to tune the optical properties of conjugated polymers, which may have potential application in light harvesting and flexible electronics.

■ ASSOCIATED CONTENT

Ⓢ Supporting Information

Synthesis of PT and rr-P3HT bottlebrushes, experimental methods, computational methodology, additional fluorescence spectra and AFM micrographs, and HOMO/LUMO and bond length/angle changes with tension. This material is available free of charge via the Internet at http://pubs.acs.org.

■ AUTHOR INFORMATION

Corresponding Author
*E-mail: sergei@email.unc.edu.

Present Address
§Department of Chemistry and Biochemistry, University of South Carolina, Columbia, SC 29208, United States (A.N.) and Department of Chemistry, University of Texas at Dallas, 800 West Campbell Road, Richardson, TX 75080, United States (M.C.S.).

Figure 5. Normalized emission spectra of rr-P3HT bottlebrushes under different backbone tensions. Inset: the corresponding energy of maximum emission as a function of backbone tension.

Notes

■ ACKNOWLEDGMENTS

■ REFERENCES

(1) Caruso, M. M.; Davis, D. A.; Shen, Q.; Odom, S. A.; Sottos, N. R.; White, S. R.; Moore, J. S. *Chem. Rev.* **2009**, *109*, 5755.
(2) Reneker, D. H.; Mattice, W. L.; Quirk, R. P.; Kim, S. J. *Smart Mater. Struct.* **1992**, *1*, 84.
(3) Ikawa, T.; Shiga, T.; Okada, A. *J. Appl. Polym. Sci.* **1997**, *66*, 1569.
(4) Yang, J.; Li, H.; Wang, G.; He, B. *J. Appl. Polym. Sci.* **2001**, *82*, 2347.
(5) Löwe, C.; Weder, C. *Adv. Mater.* **2002**, *14*, 1625.
(6) Crenshaw, B. R.; Weder, C. *Chem. Mater.* **2003**, *15*, 4717.
(7) Davis, D. A.; Hamilton, A.; Yang, J.; Cremar, L. D.; Van Gough, D.; Potisek, S. L.; Ong, M. T.; Braun, P. V.; Martinez, T. J.; White, S. R.; Moore, J. S.; Sottos, N. R. *Nature* **2009**, *459*, 68.
(8) Pagani, G.; Green, M. J.; Poulin, P.; Pasquali, M. *Proc. Natl. Acad. Sci. U.S.A.* **2012**, *109*, 11599−11604.
(9) Tanigawa, M.; Suzuto, M.; Fukudome, K.; Yamaoka, K. *Macromolecules* **1996**, *29*, 7418.
(10) Kopyshev, A.; Galvin, C. J.; Genzer, J.; Lomadze, N.; Santer, S. *Langmuir* **2013**, *29*, 13967.
(11) Schuh, C.; Lomadze, N.; Rühe, J. r.; Kopyshev, A.; Santer, S. *J. Phys. Chem. B* **2011**, *115*, 10431.
(12) Lomadze, N.; Kopyshev, A.; Rühe, J. r.; Santer, S. *Macromolecules* **2011**, *44*, 7372.
(13) Lin, J.; Beratan, D. N. *J. Phys. Chem. A* **2004**, *108*, 5655.
(14) Parks, J. J.; Champagne, A. R.; Costi, T. A.; Shum, W. W.; Pasupathy, A. N.; Neuscamman, E.; Flores-Torres, S.; Cornaglia, P. S.; Aligia, A. A.; Balseiro, C. A.; Chan, G. K.-L.; Abruña, H. D.; Ralph, D. C. *Science* **2010**, *328*, 1370.
(15) Quek, S. Y.; Kamenetska, M.; Steigerwald, M. L.; Choi, H. J.; Louie, S. G.; Hybertsen, M. S.; Neaton, J. B.; Latha, V. *Nat. Nanotechnol.* **2009**, *4*, 230.
(16) Lafferentz, L.; Ample, F.; Yu, H.; Hecht, S.; Joachim, C.; Grill, L. *Science* **2009**, *323*, 1193.
(17) Chang, S.; He, J.; Kibel, A.; Lee, M.; Sankey, O.; Zhang, P.; Lindsay, S. *Nat. Nanotechnol.* **2009**, *4*, 297.
(18) Beyer, M. K.; Clausen-Schaumann, H. *Chem. Rev.* **2005**, *105*, 2921.
(19) Neuman, K. C.; Nagy, A. *Nat. Methods* **2008**, *5*, 491.
(20) Saito, T.; Kuramae, R.; Wohlert, J.; Berglund, L. A.; Isogai, A. *Biomacromolecules* **2012**, *14*, 248.
(21) Yang, Q.-Z.; Huang, Z.; Kucharski, T. J.; Khvostichenko, D.; Chen, J.; Boulatov, R. *Nat. Nanotechnol.* **2009**, *4*, 302.
(22) Panyukov, S. V.; Sheiko, S. S.; Rubinstein, M. *Phys. Rev. Lett.* **2009**, *102*, 148301.
(23) Guérin, G. r.; Wang, H.; Manners, I.; Winnik, M. A. *J. Am. Chem. Soc.* **2008**, *130*, 14763.
(24) Wang, X.; Guerin, G.; Wang, H.; Wang, Y.; Manners, I.; Winnik, M. A. *Science* **2007**, *317*, 644.
(25) Lebedeva, N. V.; Sun, F. C.; Lee, H.-i.; Matyjaszewski, K.; Sheiko, S. S. *J. Am. Chem. Soc.* **2008**, *130*, 4228.
(26) Li, Y.; Nese, A.; Matyjaszewski, K.; Sheiko, S. S. *Macromolecules* **2013**, *46*, 7196.
(27) Park, I.; Shirvanyants, D.; Nese, A.; Matyjaszewski, K.; Rubinstein, M.; Sheiko, S. S. *J. Am. Chem. Soc.* **2010**, *132*, 12487.
(28) Coakley, K. M.; McGehee, M. D. *Chem. Mater.* **2004**, *16*, 4533.
(29) Sirringhaus, H. *Adv. Mater.* **2005**, *17*, 2411.
(30) Cardin, D. J. *Adv. Mater.* **2002**, *14*, 553.
(31) Friend, R. H.; Gymer, R. W.; Holmes, A. B.; Burroughes, J. H.; Marks, R. N.; Taliani, C.; Bradley, D. D. C.; Santos, D. A. D.; Bredas, J. L.; Logdlund, M.; Salaneck, W. R. *Nature* **1999**, *397*, 121.
(32) Yang, L.; Zhang, T.; Zhou, H.; Price, S. C.; Wiley, B. J.; You, W. *ACS Appl. Mater. Interfaces* **2011**, *3*, 4075.
(33) Matyjaszewski, K.; Xia, J. *Chem. Rev.* **2001**, *101*, 2921.
(34) Lee, H.-i.; Pietrasik, J.; Sheiko, S. S.; Matyjaszewski, K. *Prog. Polym. Sci.* **2010**, *35*, 24.
(35) Matyjaszewski, K. *Macromolecules* **2012**, *45*, 4015.
(36) Xu, H.; Sheiko, S. S.; Shirvanyants, D.; Rubinstein, M.; Beers, K. L.; Matyjaszewski, K. *Langmuir* **2005**, *22*, 1254.
(37) Berggren, M.; Bergman, P.; Fagerström, J.; Inganäs, O.; Andersson, M.; Weman, H.; Granström, M.; Stafström, S.; Wennerström, O.; Hjertberg, T. *Chem. Phys. Lett.* **1999**, *304*, 84.
(38) Nilsson, K. P. R.; Rydberg, J.; Baltzer, L.; Inganäs, O. *Proc. Natl. Acad. Sci. U.S.A.* **2003**, *100*, 10170.
(39) Sun, F.; Sheiko, S. S.; Möller, M.; Beers, K.; Matyjaszewski, K. *J. Phys. Chem. A* **2004**, *108*, 9682.
(40) Li, Y.; Nese, A.; Lebedeva, N. V.; Davis, T.; Matyjaszewski, K.; Sheiko, S. S. *J. Am. Chem. Soc.* **2011**, *133*, 17479.
(41) Zade, S. S.; Bendikov, M. *Chem.—Eur. J.* **2007**, *13*, 3688.
(42) Balamurugan, S. S.; Bantchev, G. B.; Yang, Y.; McCarley, R. L. *Angew. Chem., Int. Ed.* **2005**, *44*, 4872.
(43) Choi, J.; Ruiz, C. R.; Nesterov, E. E. *Macromolecules* **2010**, *43*, 1964.
(44) Wang, M.; Zou, S.; Guerin, G.; Shen, L.; Deng, K.; Jones, M.; Walker, G. C.; Scholes, G. D.; Winnik, M. A. *Macromolecules* **2008**, *41*, 6993.